

# Chemistry in Disks.

## II. – Poor molecular content of the AB Aur disk. <sup>\*</sup>

Katharina Schreyer<sup>1</sup>, Stéphane Guilloteau<sup>2,3</sup>, Dmitry Semenov<sup>4</sup>, Aurore Bacmann<sup>2,3</sup>, Edwige Chapillon<sup>5</sup>, Anne Dutrey<sup>2,3</sup>, Frederic Gueth<sup>5</sup>, Thomas Henning<sup>4</sup>, Frank Hersant<sup>2,3</sup>, Ralf Launhardt<sup>4</sup>, Jérôme Pety<sup>5</sup>, Vincent Piétu<sup>5</sup>

<sup>1</sup> Astrophysikalisches Institut und Universitäts-Sternwarte, Schillergässchen 2-3 D - 07745 Jena, Germany

<sup>2</sup> Université Bordeaux I; Laboratoire d'Astrophysique de Bordeaux (LAB)

<sup>3</sup> CNRS/INSU - UMR5804 ; BP 89, F-33270 Floirac, France

<sup>4</sup> Max-Planck-Institut für Astronomie, Königstuhl 17, D-69117 Heidelberg, Germany

<sup>5</sup> IRAM, 300 rue de la piscine, F-38406 Saint Martin d'Hères, France

Received 20 December 2007 / Accepted 10 September 2008

### ABSTRACT

**Aims.** We study the molecular content and chemistry of a circumstellar disk surrounding the Herbig Ae star AB Aur at (sub-)millimeter wavelengths. Our aim is to reconstruct the chemical history and composition of the AB Aur disk and to compare it with disks around low-mass, cooler T Tauri stars.

**Methods.** We observe the AB Aur disk with the IRAM Plateau de Bure Interferometer in the C- and D- configurations in rotational lines of CS, HCN, C<sub>2</sub>H, CH<sub>3</sub>OH, HCO<sup>+</sup>, and CO isotopes. Using an iterative minimization technique, observed column densities and abundances are derived. These values are further compared with results of an advanced chemical model that is based on a steady-state flared disk structure with a vertical temperature gradient, and gas-grain chemical network with surface reactions.

**Results.** We firmly detect HCO<sup>+</sup> in the 1–0 transition, tentatively detect HCN, and do not detect CS, C<sub>2</sub>H, and CH<sub>3</sub>OH. The observed HCO<sup>+</sup> and <sup>13</sup>CO column densities as well as the upper limits to the column densities of HCN, CS, C<sub>2</sub>H, and CH<sub>3</sub>OH are in good agreement with modeling results and those from previous studies.

**Conclusions.** The AB Aur disk possesses more CO, but is less abundant in other molecular species compared to the DM Tau disk. This is primarily caused by intense UV irradiation from the central Herbig A0 star, which results in a hotter disk where CO freeze out does not occur and thus surface formation of complex CO-bearing molecules might be inhibited.

**Key words.** Stars: circumstellar matter – planetary systems: protoplanetary disks – individual: AB Aur – Radio-lines: stars

### 1. Introduction

The rich variety of the detected exoplanetary systems cannot be fully understood without knowledge about the physical and chemical evolution of their precursors – protoplanetary disks. The question what role chemistry plays during planet formation and how it is coupled to disk dynamics remains loosely constrained.

Nowadays it is widely believed that disk evolution is controlled by redistribution of angular momentum due to turbulent viscosity. A promising source of turbulence is the magnetorotational instability that works if the disk matter is sufficiently ionized (Balbus & Hawley, 1991). The chemistry of ionization fraction in protoplanetary disks was stud-

ied in detail, both theoretically and observationally (see, e.g., Gammie, 1996; Glassgold et al., 1997; Igea & Glassgold, 1999; Semenov, Wiebe, & Henning, 2004; Ilgner & Nelson, 2006; Pascucci et al., 2007). To a large extent it is dominated by stellar radiation in the upper disk region and high-energy cosmic ray particles in their midplanes. For the inner, planet-forming disk regions, X-ray radiation from a young star may play a crucial role. Recently, Turner et al. (2007) investigated the evolution of the ionization degree in the inner region of a protoplanetary disk, using a coupled 3D magneto-hydrodynamical and chemical code and found that dynamic transport increases electron concentration within the dead zone. It has been widely discussed that the interplay between chemical and transport processes must have been important during the formation of our own solar system (e.g., Cyr et al., 1998; Bockelée-Morvan et al., 2002; Wooden et al., 2005).

Due to high computational demands, the studies of disk chemistry coupled to disk dynamics are in their early stages (Ilgner et al., 2004; Willacy et al., 2006; Semenov et al., 2006;

Send offprint requests to: K. Schreyer, e-mail: martin@astro.uni-jena.de

<sup>\*</sup> Based on observations carried out with the IRAM Plateau de Bure Interferometer. IRAM is supported by INSU/CNRS (France), MPG (Germany) and IGN (Spain).

**Table 1.** List of observations using the Plateau de Bure Interferometer. In the column of the configuration, the abbreviation of e.g. “5D” refers to the number of antennas and the used configuration.

Line	transition	frequency [MHz]	configu- ration	baseline range [m]	integration time ( $T_{\text{ON}}$ ) [h]	synthesized beam size, position angle	1 $\sigma$ rms [mJy/beam]
HCO <sup>+</sup>	1–0	89188.523	5D,C2	24 – 175	5.9+10	5.2'' $\times$ 4.8'', 6°	18
HCN	$J=1-0, F=2-1$	88631.847	6CD	24 – 175	5.9	6.0'' $\times$ 4.2'', 105°	24
CS	2–1	97980.950	5D	24 – 160	1.8	9.0'' $\times$ 4.2'', 120°	170
C <sub>2</sub> H	$N=1-0, J=3/2-1/2, F=2-1$	87316.925	6D	24 – 113	1	9.8'' $\times$ 3.9'', 110°	37
CH <sub>3</sub> OH	15 <sub>(3,13)</sub> –14 <sub>(4,10)</sub> A <sup>+</sup>	88594.960	6CD	24 – 175	3.9	6.1'' $\times$ 4.2'', 105°	24
CH <sub>3</sub> OH	15 <sub>(3,12)</sub> –14 <sub>(4,11)</sub> A <sup>–</sup>	88940.090	5D	24 – 175	3.9+2.2	6.3'' $\times$ 4.3'', 105°	24
CH <sub>3</sub> OH	2 <sub>(1,1)</sub> –1 <sub>(1,0)</sub> A <sup>–</sup>	97582.830	5D	32 – 73	1.8	9.4'' $\times$ 4.3'', 148°	170

Tscharnuter & Gail, 2007). Chemical models were successfully applied to study disk chemistry for steady-state accretion disks (e.g., Willacy et al., 1998; van Dishoeck & Blake, 1998; Aikawa & Herbst, 1999; Markwick et al., 2002; Semenov et al., 2005; Dutrey et al., 2007). The most important result is the chemical stratification in such disks, where many molecules are abundant at an intermediate, slightly UV irradiated layer, while being frozen out in the cold and dark midplane and broken apart by unshielded high-energy radiation in disk atmospheres. Bergin et al. (2003) have shown that the non-thermal UV radiation from T Tauri stars may partly come in Ly $\alpha$  photons, which significantly affects abundances of molecules dissociated by these photons. In contrast, Herbig Be/Ae stars emit much stronger thermal UV radiation, with circumstellar disks being hotter and more ionized than the disks around T Tauri stars.

A detailed understanding of physical and chemical conditions of the planet-forming environment requires not only sophisticated models, but also high-resolution observations of protoplanetary disks, both in dust continuum and various molecular lines. Unfortunately, such studies are challenging due to the limited sensitivity and spatial resolution of available observational facilities, and small disk sizes ( $\sim 100 - 1000$  AU). Dutrey et al. (1997) and Kastner et al. (1997) have first detected several molecular species towards protoplanetary disks by using the IRAM 30m single-dish telescope, followed by observations of van Zadelhoff et al. (2001); Thi et al. (2004); Semenov et al. (2005). Interferometric observations by Qi (2001); Aikawa et al. (2003); Piétu et al. (2006, 2007) allowed to study disk gas at outer radii  $\geq 50$  AU in lines of several abundant species (CO, <sup>13</sup>CO, C<sup>18</sup>O, HCO<sup>+</sup>, CS, CN, H<sub>2</sub>CO). These studies have confirmed that photochemistry plays an important role even at large disk radii and that abundances of many gas-phase molecules are depleted.

In 2005 a joint Heidelberg-Bordeaux “Chemistry In Disks” (CID) project was established to investigate the spatial distribution of various molecular tracers across well-studied T Tauri and Herbig Ae disks of various age, followed by comprehensive modeling. In the first paper of this series, we have presented the results of a deep search for N<sub>2</sub>H<sup>+</sup> and HCO<sup>+</sup> towards two T Tauri stars (DM Tau, LkCa 15) and one Herbig Ae star (MWC 480), see Dutrey et al. (2007). The N<sub>2</sub>H<sup>+</sup> emission has been detected in LkCa 15 and DM Tau, with the N<sub>2</sub>H<sup>+</sup> to HCO<sup>+</sup> ratio similar to that of cold dense cores and the disk ionization degree as predicted by chemi-

cal models. In this second paper, we investigate the molecular content of the well-studied disk around the Herbig Ae star AB Aurigae (van den Ancker et al., 1998; Grady et al., 1999; Roberge et al., 2001; Fukagawa et al., 2004, distance = 145 pc), which is an intermediate-mass analog of the young T Tauri stars and evolutionary precursor of the main-sequence debris disk sources like  $\beta$  Pic,  $\alpha$  Lyr, and  $\alpha$  PsA. This disk is peculiar in comparison with other known circumstellar disks since it is still embedded in a rather extended envelope and has clumpy density sub-structures (Fukagawa et al., 2004; Corder et al., 2005; Piétu et al., 2005; Lin et al., 2006). This points toward a low-mass companion or a giant planet (Rodríguez et al., 2007), a recent stellar encounter, or imprint of earlier non-steady evolution (see discussion in Piétu et al. (2005), hereafter Paper II). Using the IRAM 30-m telescope, Semenov et al. (2005, hereafter Paper I) have studied the molecular content towards this source at low resolution and derived basic parameters of the envelope. They have derived a low disk inclination of about 17° (face-on orientation) and low disk mass of about 0.013  $M_{\odot}$ . Piétu et al. (2005) have resolved the disk structure in different CO isotopes using the Plateau de Bure Interferometer (PdBI). They have found that the disk is inclined by about 30° and its rotation departs from the Keplerian law, with an exponent for the rotation velocity as low as 0.41. The outer radius of the gaseous disk is close to  $\sim 1000$  AU, its inner hole is at a radius of  $\approx 100$  AU in the dust emission, and at  $\approx 70$  AU in CO lines, and the disk mass is  $\approx 0.02 M_{\odot}$ .

The main aim of the present study is to search for C<sub>2</sub>H, CS, HCN, HCO<sup>+</sup>, CH<sub>3</sub>OH, and CO isotopes in the disk of AB Aur using compact interferometer configurations of the PdBI, to derive their column densities, and to compare these values with those from a robust chemical model and the disk of a cooler T Tauri star DM Tau.

## 2. Observations

Observations with the PdBI were carried out between February and August 2002 using the compact C and D configurations and single side band tuning. Table 1 lists the observational parameters for the individual observing runs.

The frequencies are taken from the Cologne Database for Molecular Spectroscopy (Müller et al., 2001, 2005). The phase reference center is RA(2000) = 04<sup>h</sup> 55<sup>m</sup> 54.8<sup>s</sup>; DEC(2000) = +30° 33' 04.3''. All line observations were performed in the lower side band with a frequency resolution of 39 kHz, lead-

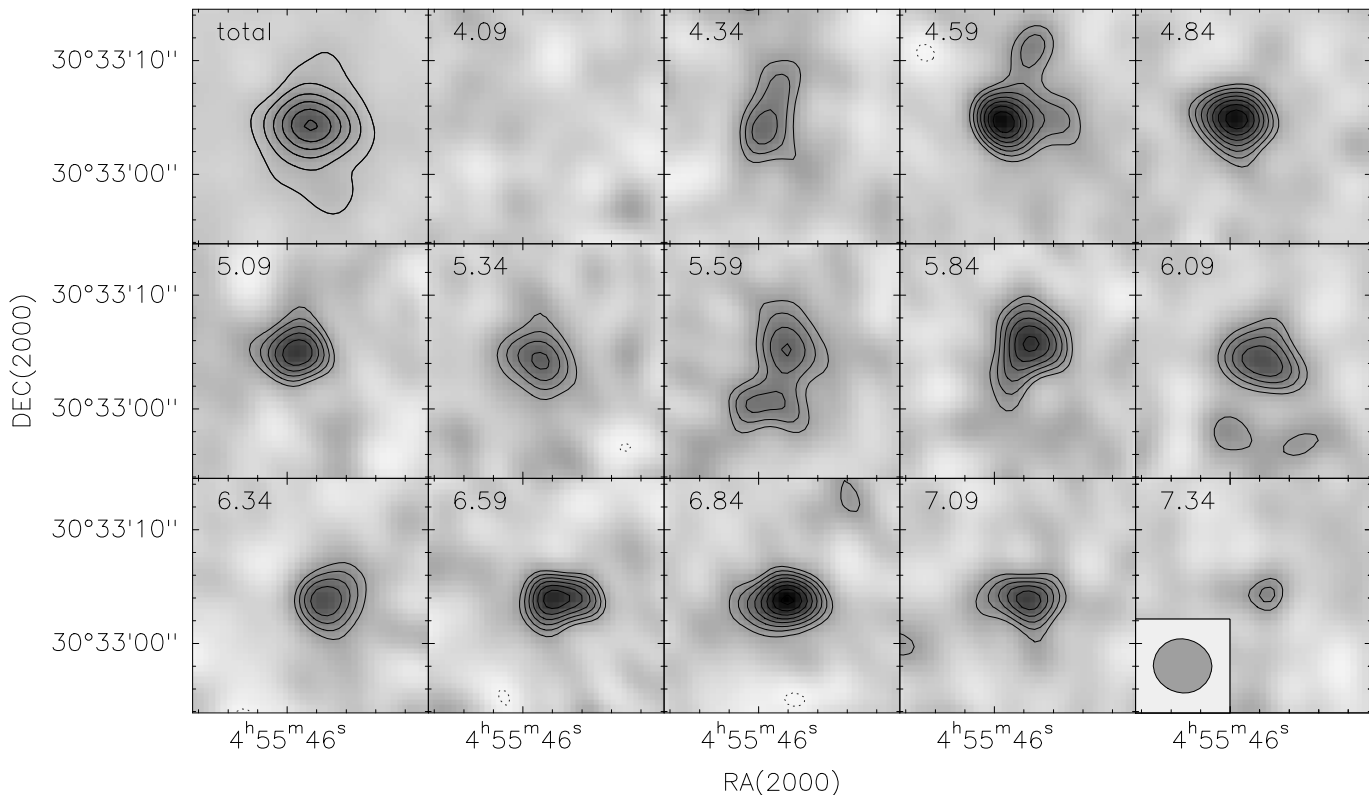


**Fig. 1.** Mapping results of the combined  $\text{HCO}^+$  (1–0) data. Contour levels are:  $-0.04$  to  $0.13 \text{ Jy km s}^{-1}$  in step of  $0.04 \text{ Jy km s}^{-1}$ . The mean velocity of each channel is given in each box top left. In the panel top left, the total integrated  $\text{HCO}^+$  map is shown. Contour levels are:  $-0.015$  to  $7.010 \text{ Jy km s}^{-1}$  in step of  $0.015 \text{ Jy km s}^{-1}$ . The area of the HPBW of the synthesized beam is indicated as a grey ellipse in the panel bottom right.

ing to a velocity resolution of  $0.14 \text{ km s}^{-1}$ . We took advantage of the flexible correlator to observe simultaneously transitions of  $\text{CH}_3\text{OH}$  in the same bandpass as for the observations of  $\text{HCO}^+$ ,  $\text{CS}$ , and  $\text{HCN}$ . The total integration time was rather short, about 2 hours for each line. We combined the  $\text{HCO}^+$  (1–0) data obtained during these observations with that from Paper II to reconstruct the final image at  $5.34'' \times 4.8''$  spatial resolution.

The bandpass and phase calibration were performed using observations of the objects 3C84, 3C345, MWC349, CRL 618, and 0528+134. The GILDAS software is utilized for the data reduction and final phase calibration. The resulting synthesized half-power beam widths are listed in Table 1.

All listed lines in Table 1 were centered to the systemic velocity of  $V_{\text{LSR}} = 5.8 \text{ km s}^{-1}$ . The weak underlying continuum was detected, with an integrated  $\lambda 3 \text{ mm}$  flux of  $3.7 \text{ mJy}$ . This is consistent with previous measurements of Piétu et al. (2005). For the final analysis of the observed line spectra this continuum was subtracted.

### 3. Results

The transition of  $\text{HCO}^+$  (1–0) was the only spectral line that was well detected in each observing run. In Figs. 1 and 2 we show the combined spectrum of  $\text{HCO}^+$  (1–0). With the beam of  $5.34'' \times 4.8''$ , that is comparable to the disk size, we do not fully resolve the disk around AB Aur (Fig. 1, upper left panel).

However, the pattern typical for rotating circumstellar disks appears clearly in various channel maps (Fig. 1). The peak intensity of the double line profile of  $\text{HCO}^+$  is  $0.12 \text{ Jy/beam}$ , which is 10 times higher than the noise level. Fig. 2 shows the variation of the line profiles across the spatial extent of the AB Aur disk, which is similar to the spectra presented in Papers I/II. The symmetric double-peaked line profile at the center of the spectral map is a typical feature of barely resolved Keplerian disks. Since deconvolution is a highly non-linear procedure that is prone to errors we perform our analysis in the  $uv$ -space, using the  $\chi^2$ -minimization technique of Guilloteau & Dutrey (1998).

None of the other attempted species were detected ( $\text{C}_2\text{H}$ ,  $\text{CS}$ , and  $\text{CH}_3\text{OH}$ ), but we have a hint of the  $\text{HCN}$  (1–0) hyperfine line components  $F = 1-1$  and  $F = 2-1$  at the  $2\sigma$  noise level. The  $1\sigma$  rms noise levels for all species are listed in Table 1.

To better quantify the column densities and molecular abundances, we analyze the data by applying the parametric disk model and the  $\chi^2$ -minimization method as described in Guilloteau & Dutrey (1998). First, we analyze the  $\text{HCO}^+$  data leaving as many free parameters as possible. This allows us to verify the compatibility of the  $\text{HCO}^+$  emission with the disk parameters derived from the CO isotopologues in Paper II. The disk parameters derived from Paper II and found from  $\text{HCO}^+$  are presented in Table 2.

Although the angular resolution is low, the  $\text{HCO}^+$  data confirms one important point: the existence of the inner hole of

$\simeq 75 - 100$  AU radius found in Paper II. This hole manifests itself as a lack of emission at projected velocities beyond  $\pm 1.6$  km s $^{-1}$  from the systemic velocity, but the hole is not directly visible in the spectral map. The temperature is not well constrained from HCO $^{+}$ , but compatible with that found from CO isotopologues. Overall, the non-Keplerian motion detected in Paper II seems less obvious in the HCO $^{+}$  data: the best fit inclination is slightly lower, giving a rotation velocity more in agreement with the stellar mass. Since our low angular resolution data masks out HCO $^{+}$  emission from inner, highly inhomogeneous disk regions, the corresponding velocity profile seems to be closer to a Keplerian law. However, if the inner radius is fixed to 75 AU, the velocity index derived from HCO $^{+}$  becomes  $0.36 \pm 0.04$ , in agreement with Paper II.

We use derived disk parameters (Col. 2 in Table 2) to determine column densities for all observed molecules. The derived column density of HCO $^{+}$  and upper limits for other species are summarized in Table 4. These column densities scale linearly with the assumed temperature, but are independent from any of the other parameters.

#### 4. Modeling

As a next step, we try to reproduce the measured column densities and the upper limits altogether using an advanced disk physical model and the chemical structure from a robust chemical model, similar to Paper I. The overall iterative fitting is easier than in Paper I since we refrain from comparing deconvolved observed and simulated spectral maps and base our analysis on the observed quantities derived with the  $\chi^2$ -minimization method in the  $uv$ -plane. This allows us to exclude computationally expensive radiative transfer modeling with beam convolution from consideration.

To simulate the disk physical structure we utilize a passive flared 2D disk model of Dullemond & Dominik (2004) with a vertical temperature gradient and non-grey dust opacities. Some input disk and stellar parameters are taken as determined by the  $\chi^2$ -fitting or found in previous works (van den Ancker et al., 1998; Thi et al., 2004; Piétu et al., 2005; Semenov et al., 2005), see Table 2. Other key parameters, like the radial slope of surface density, the disk mass, and the cosmic ray ionization rate, are found by iterative fitting of the observed data (Table 3).

We assume that the central A0e star has an effective temperature of 10 000 K, a radius of  $2.5R_{\odot}$ , and a mass of 2.4 solar masses (van den Ancker et al., 1998, 2000). The dust grains are modeled as compact spheres of uniform  $0.12 \mu\text{m}$  radius made of pure amorphous silicates with the optical data taken from Draine & Lee (1984). The standard 1% dust-to-gas mass ratio is used. Utilizing the results of Papers I and II, the disk inner radius is assumed to be  $\sim 70$  AU, the outer radius is 1 100 AU, and the disk age is between 2 and 5 Myr.

The disk is illuminated by the UV radiation from the central star and by the interstellar UV radiation. The intensity of the un-attenuated stellar UV flux is calculated using the Kurucz (1993) ATLAS9 of stellar spectra and converted to the  $\chi_{*} = 10^5 \chi$  factor at 100 AU, where the factor  $\chi$  is the mean interstellar UV field of Draine (1978). The UV intensity at a given

**Table 2.** List of disk and stellar parameters using the  $\chi^2$  minimization in the UV plane

	disk parameters derived from	
	$^{13}\text{CO}$ (Paper II)	HCO $^{+}$ (this paper)
$V_{\text{LSR}}$ (km s $^{-1}$ )	5.87	$5.87 \pm 0.03$
Inclination ( $^{\circ}$ )	35	$21 \pm 16$
$V \sin(i)$ (km s $^{-1}$ )	1.67	$1.49 \pm 0.07$
Velocity exponent	0.40	$0.40 \pm 0.04$
Position angle ( $^{\circ}$ )	-30	$-20 \pm 4$
Inner radius (AU)	75	$110 \pm 16$
Outer radius (AU)	1000	$> 800$
Temperature (K)	35	[35]
exponent q	0.1	[0.1]
Column density (cm $^{-2}$ )	$6.2 \times 10^{22}$	$6.2 \pm 1.2 \cdot 10^{12}$
exponent	2.5	$3.5 \pm 0.5$
Line width (km s $^{-1}$ )	0.40	$0.23 \pm 0.10$

The fixed parameters are taken from Table I of Paper II, as an average of the results from the  $^{13}\text{CO}$ . The column density is for H $_2$  (Col 2) and HCO $^{+}$  (Col 3) at 250 AU.

**Table 3.** List of disk and stellar parameters used in the best-fit model

Parameter	Dimension	Fixed	Derived
Stellar radius	$R_{\odot}$	2.5	...
Stellar mass	$M_{\odot}$	2.4	...
Effective temperature	K	10 000	...
Stellar UV RF at 100 AU	$\chi_0$	100 000	...
CRP ionization rate	s $^{-1}$	...	$4 \cdot 10^{-18}$
Inner disk radius	AU	70	...
Outer disk radius	AU	1 100	...
Disk mass	$M_{\odot}$	...	0.02
Surface density profile	...	...	-2.15
Grain size	$\mu\text{m}$	0.12	...
Dust-to-gas mass ratio	...	0.01	...

The fixed stellar and disk parameters are taken from Piétu et al. (2005).

disk location is calculated as a sum of the stellar and interstellar components that are scaled down by the visual extinction in vertical direction and in direction to the central star (1D plane-parallel approximation). We model the attenuation of cosmic rays (CRP) by Eq. (3) from Semenov, Wiebe, & Henning (2004) and vary the initial value of the ionization rate  $\zeta_{\text{CRP}}$  between about  $10^{-18}$  and  $10^{-17}$  s $^{-1}$  to match the HCO $^{+}$  data. In the disk interior, ionization due to the decay of short-living radionuclides is taken into account, assuming an ionization rate of  $6.5 \cdot 10^{-19}$  s $^{-1}$  (Finocchi & Gail, 1997). The stellar X-ray radiation is assumed to be weak in intermediate-mass stars due to a lack of the dynamo mechanism and thus is neglected. Though the observed X-ray luminosity of the AB Aur is non-negligible, its spectrum is dominated by soft photons with energies below  $\sim 1$  keV (Telleschi et al., 2007), which cannot penetrate easily deep into the disk.

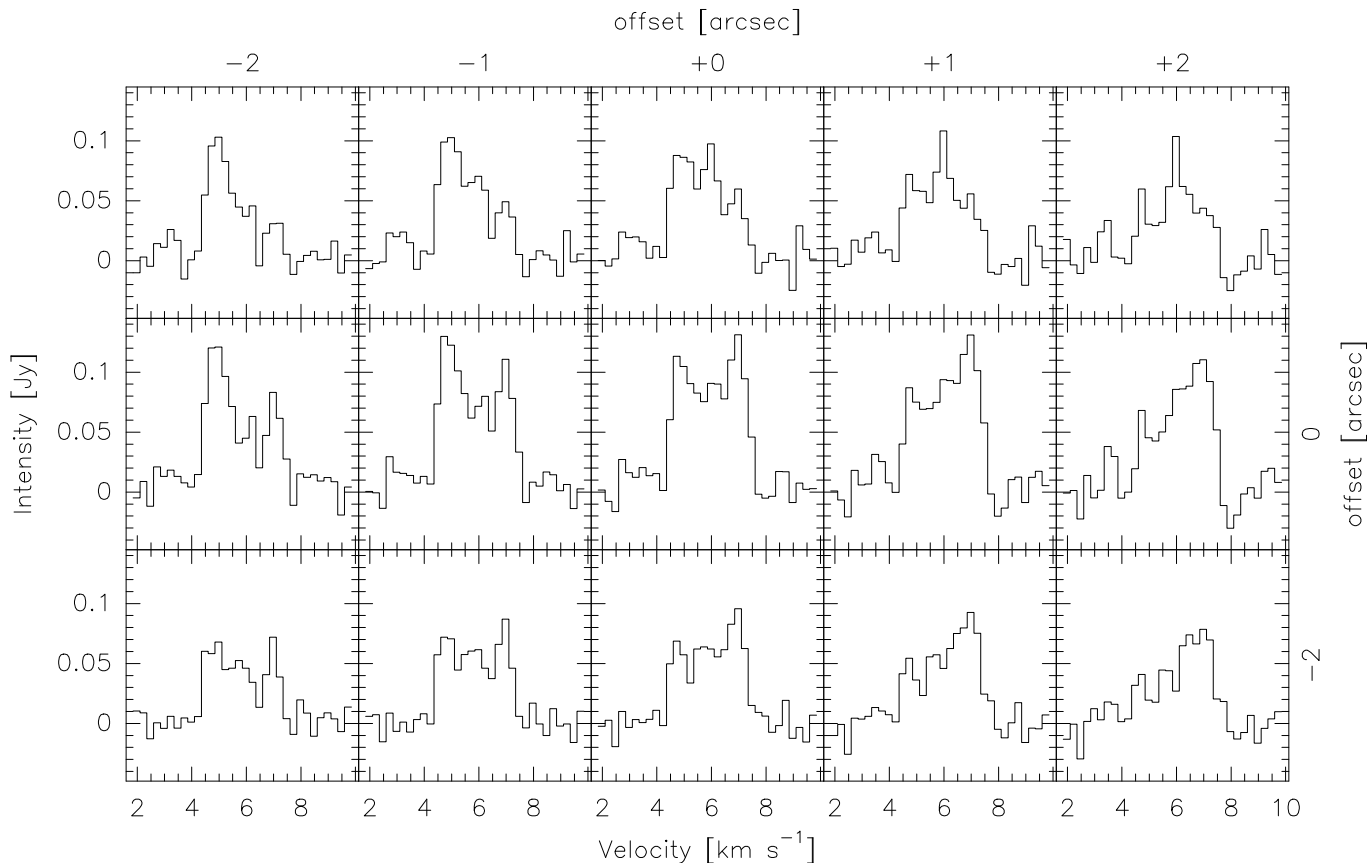


**Fig. 2.** Spatial variation of the  $\text{HCO}^+$  (1–0) line profiles across the AB Aur disk.

The gas-grain time-dependent chemical model adopted in this study is mostly the same as in Paper I, but with two major modifications. First, we now use *osu.2007*, the latest version of the Ohio State University (OSU) database of gas-phase reactions<sup>1</sup> (Smith et al., 2004), with all recent updates to the reaction rates. Second, we utilize a standard rate approach to the surface chemistry modeling but without H and  $\text{H}_2$  quantum tunneling (Katz et al., 1999). So, only thermal hopping of surface reactants is allowed. The surface reactions together with desorption energies are taken from Garrod & Herbst (2006), which is mostly based on previous studies of Hasegawa et al. (1992) and Hasegawa & Herbst (1993). Finally, rates of several tens of photodissociation and photoionization reactions are updated according to van Dishoeck et al. (2006), using the UV spectral shape typical of a Herbig Ae star and the ISM-like dust grain optical properties.

Overall, the disk chemical network consists of about 650 species made of 13 elements and 7300 reactions. Using this time-dependent chemical model, distributions of the molecular abundances and column densities for the considered species are simulated over 5 Myr of evolution.

## 5. Results and Discussion

The Fig. 3 shows the calculated 2D abundance distribution for all observed molecular species. The vertical scale is given

in units of pressure scale height calculated for the midplane temperature (Dartois, Dutrey, & Guilloteau, 2003). The corresponding vertically integrated column densities versus the radius are shown and also listed in Table 4. This best-fit physico-chemical model of the AB Aur disk is obtained after about 20 iterations by varying the cosmic ray ionization rate, total disk mass, and surface density exponent. All values refer to a radius of 250 AU. Upper limits for CS and  $\text{CH}_3\text{OH}$  were derived using the  $2\sigma$  errors of the  $\chi^2$ -minimization. For these estimates, the  $\text{H}_2$  column density of  $N(\text{H}_2) = 6.2 \times 10^{22} \text{ cm}^{-2}$  was adopted from Paper II as a reference. We have adopted an  $^{13}\text{C}/^{12}\text{C}$  isotopic ratio of 70.

In agreement with previous studies and the observations of T Tauri disks, chemical stratification is apparent in the disk around AB Aur (see Fig. 5 in Dutrey et al., 2007). The disk surrounding the central A0e star is hotter and has a warm midplane ( $T \gtrsim 20 \text{ K}$ ) and, therefore, CO molecules do not freeze out while other molecules do. Due to self-shielding, energetic UV radiation from AB Aur cannot dissociate a large fraction of CO. This leads to a high CO column density of about  $3 \times 10^{18} \text{ cm}^{-2}$  at 250 AU, with a relative CO abundance of  $7 \times 10^{-5}$ . It seems that such a low surface CO population in the disk of AB Aur may lead to inhibited catalytic formation of complex molecules like methanol via hydrogen addition reactions on dust surfaces. In contrast, in the DM Tau disk a substantial fraction of CO resides on dust grains, so that the averaged relative CO abundance in the gas phase is 6 times lower,  $\sim 10^{-6}$ . We found that, within adopted disk masses of  $0.001 - 0.1 M_{\text{sun}}$ , the radial pro-

<sup>1</sup> See: <https://www.physics.ohio-state.edu/eric/research.html>

file of the CO column density obtained by chemical modeling strictly follows the input surface density profile with a scaling factor.

The chemically related molecular ion,  $\text{HCO}^+$ , is directly produced from CO by ion-molecule reactions with  $\text{H}_3^+$  and gets destroyed by dissociative recombination. In turn, formation of  $\text{H}_3^+$  is solely due to interactions of cosmic ray particles with molecular hydrogen (see e.g., Oka, 2006). Thus, the  $\text{HCO}^+$  column density is sensitive to adopted cosmic ray ionization rate and, to some extent, temperature structure. Our best-fit model reproduces the observed  $\text{HCO}^+$  column density at 250 AU,  $6 \cdot 10^{12} \text{ cm}^{-2}$ , within a factor of 2.5 ( $N_{\text{mod}}(\text{HCO}^+) \approx 10^{13} \text{ cm}^{-2}$ ), which is comparable to observational and inherent chemical uncertainties (Vasyunin et al., 2008).

In contrast to the DM Tau disk where  $\text{HCO}^+$  is mostly concentrated in the intermediate layer due to freeze out of CO,  $\text{HCO}^+$  reaches the highest concentration in the midplane of the AB Aur disk. The  $\text{HCO}^+$  ion was found to be very sensitive to the adopted value of the CRP flux and radial density distribution. The acceptable fit to observations was only possible when the CRP ionization rate was lowered by a factor of 3–5 compared to the standard value of  $1.3 \cdot 10^{-17} \text{ s}^{-1}$ , the surface density profile is  $\approx -2.15$ , and the disk mass is between  $0.008 - 0.012 M_{\text{sun}}$ . With lower disk masses, the predicted  $^{13}\text{CO}$  column density was lower than the observed value ( $4 \cdot 10^{16} \text{ cm}^{-2}$  at 250 AU), while with other density profiles it was impossible to get proper CS,  $\text{C}_2\text{H}$  and HCN column densities. The model results dependent on the adopted inner radius – with radii smaller than about 50 AU and fixed total disk mass the modeled  $\text{HCO}^+$  and CO concentrations were lower than the observed values. As we used the newly measured inner radius of  $\sim 70$  AU (see paper II), it is not surprising that the modeled distribution of  $\text{HCO}^+$  in the AB Aur disk differs from the results of Paper I (see Fig. 5 therein).

The reason why the CRP ionization rate could be lower in AB Aur than a widely accepted value ( $\approx 10^{-17} \text{ s}^{-1}$ ) is many-fold. First of all, the standard ionization rates of He and  $\text{H}_2$  can be uncertain by a factor of 2 (Wakelam et al., 2006). Second, if a self-generation of magnetic fields in protoplanetary disks by a dynamo-like mechanism takes place (Dolginov & Stepinski, 1994), then the cosmic ray particles will be scattered and will not reach disk midplanes – exactly the zone where a significant fraction of  $\text{HCO}^+$  exists in the AB Aur disk. Third, the AB Aur disk has a complex and clumpy structure (Fukagawa et al., 2004; Piétu et al., 2005; Lin et al., 2006), and, consequently, efficiency of dissociative recombination of  $\text{HCO}^+$  will be different in clumps compared to an inter-clump medium. Our axisymmetric disk model does not take this effect into account. Last, there may be some missed important reaction pathways to  $\text{HCO}^+$  or improperly derived reactions rates.

Abundances and column densities of other observed molecules are also explained by this model. The chemically active  $\text{C}_2\text{H}$  radical is only abundant in dilute, irradiated disk surface and quickly converted into heavier, more complex species in the denser region adjacent to the midplane (Fig. 3). On the other hand, HCN and CS are more widely distributed across the AB Aur disk, though both these molecules are underabundant in the midplane where they stick to grains and surface pro-

cessed. Note that the column densities of CO and thus  $\text{HCO}^+$  decrease with radius, whereas the column densities of  $\text{C}_2\text{H}$  and HCN slightly increase with radius. The CS column density stays nearly constant for large radii,  $r \gtrsim 200$  AU, and is found to be stable against iterative variations of the input parameters. It is HCN that depends on the adopted value of the surface density exponent. As this molecule can be easily photodissociated by stellar UV photons, its abundance is sensitive to details of the disk vertical structure, in particular, shielding by dust. Presumably, all modeled column densities agree well with the observed values or upper limits due to the lack of sensitivity of the measurements. On the other hand, the derived radial profiles are shallower than extracted from observations by the  $\chi^2$ -minimization analysis. The surface density is a measure of the total disk mass, which is usually obtained from thermal dust emission and poorly known dust properties (gas-to-dust ratio, opacities), and thus can be rather uncertain (see discussion in Paper I).

It is interesting to compare the molecular contents of the AB Aur disk and of another well-studied disk around the T Tauri star DM Tau. The DM Tau disk has a similar size of  $\sim 1000$  AU with a hole of a few AU in size (Calvet et al., 2005), is more evolved ( $\sim 5$  Myr), and more massive ( $\sim 0.05 M_{\odot}$ ) (see Table 2 in Dutrey et al., 2007). In Table 4 the observed column densities rescaled to the  $^{13}\text{CO}$  value at 250 AU are listed for the DM Tau disk as well (last column). These rescaled values are less sensitive to possible errors in the estimate of the disk mass and surface density.

It is apparent that relative column densities for all observed species are lower in the disk of AB Aur compared to the values observed in the DM Tau disk. Given that the absolute column density of  $^{13}\text{CO}$  at 250 AU is similar in both disks, it implies a poor molecular content of the AB Aur disk (except of CO and  $\text{H}_2$ ). However, the disk around DM Tau is about 4 times more massive than the AB Aur disk. The fact that both disks harbor similar amounts of CO despite significant difference in their masses is likely a direct manifestation of severe freeze out in the cold midplane of the DM Tau source and/or difference in grain properties.

The lower mass of the hotter AB Aur disk is likely the reason for its molecule-deficient gas content. Since the total dust shielding is lower, while the UV luminosity of the Herbig A0 star is orders of magnitude higher than that of DM Tau, the photodissociation of many molecules is more effective in the disk around AB Aur. The age difference between the two sources is a negligible factor for the results of chemical modeling, even though gas-grain models usually do not reach a steady-state within a few Myr. The same is true for surface chemistry, which is not much of importance for most of the observed species, apart from methanol.

## 6. Conclusions and Summary

The AB Aur environment is clearly dominated by the envelope, as shown by the detections made with the 30-m telescope and the lack of detections with the IRAM array in short (1-3 hours) integrations. The disk has an inner hole in the gas distribution with a radius of  $\approx 70$  AU. Using a gas-grain chemical model

**Table 4.** Observed and modeled column densities  $N$  in AB Aur and DM Tau.

Molecule	$\chi^2$ -minimization method			Chemical model		DM Tau
	N [cm <sup>-2</sup> ]	1 $\sigma$ error	N/N( <sup>13</sup> CO) <sup>(1*)</sup>	N [cm <sup>-2</sup> ]	N/N( <sup>13</sup> CO) <sup>(2*)</sup>	N/N( <sup>13</sup> CO) <sup>(1*)</sup>
H <sub>2</sub>	6 10 <sup>22</sup>	1 10 <sup>22</sup>	1.5 10 <sup>6</sup>	5 10 <sup>22</sup>	1.3 10 <sup>6</sup>	1 10 <sup>7</sup>
<sup>13</sup> CO <sup>(*)3</sup>	4 10 <sup>16</sup>	5 10 <sup>15</sup>	1	4 10 <sup>16</sup>	1	1
HCO <sup>+</sup>	6 10 <sup>12</sup>	3 10 <sup>11</sup>	1.5 10 <sup>-4</sup>	1.5 10 <sup>13</sup>	4 10 <sup>-4</sup>	2 10 <sup>-3</sup>
HCN	5 10 <sup>11</sup>	3 10 <sup>11</sup>	1.3 10 <sup>-5</sup>	4 10 <sup>11</sup>	10 <sup>-5</sup>	7 10 <sup>-4</sup>
CS	3 10 <sup>12</sup>	3 10 <sup>12</sup>	< 8 10 <sup>-5</sup>	2 10 <sup>11</sup>	5 10 <sup>-6</sup>	3 10 <sup>-4</sup>
C <sub>2</sub> H	2 10 <sup>13</sup>	2 10 <sup>13</sup>	< 5 10 <sup>-4</sup>	10 <sup>10</sup>	2.5 10 <sup>-7</sup>	10 <sup>-3</sup>
CH <sub>3</sub> OH	0	7 10 <sup>15</sup>	< 2 10 <sup>-1</sup>	0	0	0

<sup>(1\*)</sup> Relative to the <sup>13</sup>CO column density at 250 AU obtained by the  $\chi^2$ -minimization method,

<sup>(2\*)</sup> Relative to the <sup>13</sup>CO column density at 250 AU obtained by the chemical modeling,

<sup>(3\*)</sup> see results reported by Pietu et al. (2005).

with surface reactions coupled to a flared passive disk model, we reproduce all observed column densities and upper limits. Note that such a comparison between the advanced chemical model and the interferometric observations are hampered by the lack of knowledge on the H<sub>2</sub> surface density. The surface density of the AB Aur disk is derived from the millimeter dust emission, a procedure prone to uncertainties. Part of the discrepancies between the model and the observations may also be due to inhomogeneous structure of the AB Aur disk and/or grain evolution in central disk regions that is not considered in the calculations. Modeled and observed column densities relative to <sup>13</sup>CO are both lower for the AB Aur disk than the values measured in DM Tau. The absolute amounts of CO gas are similar in both disks. The poor molecular content of the AB Aur system can be explained by much more intense UV irradiation by the central A0 star and less effective dust shielding in the low-mass disk compared to the more massive disk around the less luminous M1 star DM Tau. The indirectly inferred cosmic ray ionization rate that is needed to fit the HCO<sup>+</sup> data is a factor of 2–5 lower than the standard value, which can be explained by scattering of CRPs in a magnetized AB Aur disk or a clumpy disk structure.

*Acknowledgements.* We acknowledge all the Plateau de Bure IRAM staff for their help during the observations. SG, AD, VW, FH, and VP are financially supported by the French Program “Physique Chimie du Milieu Interstellaire” (PCMI).

## References

- Aikawa, Y., & Herbst, E. 1999, A&A, 351, 233  
Aikawa, Y., Momose, M., Thi, W.-F., van Zadelhoff, G.-J., Qi, C., Blake, G.A., & van Dishoeck, Ewine F. 2003, PASJ 55, 11  
Balbus, S. A., & Hawley, J. F. 1991, ApJ, 376, 214  
Bergin, E., Calvet, N., D’Alessio, P., & Herczeg, G. J. 2003, ApJ, 591, L159  
Bockelée-Morvan, D., Gautier, D., Hersant, F., Huré, J.-M., & Robert, F. 2002, A&A 384, 1107  
Calvet, N., D’Alessio, P., Watson, D. M., et al. 2005, ApJ, 630, L185  
Corder, S., Eisner, J., & Sargent, A. 2005, ApJ, 622, 133  
Cyr, K.E., Sears, W.D., & Lunine, J.I. 1998, Icarus 135, 537  
D’Alessio, P., Calvet, N., Hartmann, L., Lizano, S., & Cantó, J. 1999, ApJ, 527, 893  
Dartois, E., Dutrey, A., & Guilloteau, S. 2003, A&A, 399, 773  
Dolginov, A. Z., & Stepinski, T. F. 1994, ApJ, 427, 377  
Draine, B.T. 1978 ApJS, 36, 595  
Draine, B.T., & Lee, H. 1984, ApJ, 285, 89  
Dullemond, C., & Dominik, C. 2004, A&A, 417, 159  
Dutrey, A., Henning, Th., Guilloteau, S., Semenov, D., Pietu, V., Schreyer, K., Bacmann, A., Launhardt, R., Pety, J., & Gueth, F. 2007, A&A, 317, L55  
Dutrey, A., Guilloteau, S., & Guelin, M. 1997, A&A, 317, L55  
Finocchi, F., & Gail, H.-P. 1997, A&A, 327, 825  
Fukagawa, M., Hayashi, M., Tamura, M., et al. 2004, ApJ, 605, L53  
Garrod, R. T., & Herbst, E. 2006, A&A 457, 927  
Gammie, C. F. 1996, ApJ, 457, 355  
Glassgold, A. E., Najita, J., & Igea, J. 1997, ApJ, 480, 344  
Grady, C. A., Woodgate, B., Bruhweiler, F. C., et al. 1999, ApJ, 523, 151  
Guilloteau, S., & Dutrey, A. 1998, A&A, 339, 467  
Hasegawa, T.I., & Herbst, E. 1993 MNRAS, 263, 223  
Hasegawa, T. I., Herbst, E., & Leung, C. M. 1992, ApJS 82, 167  
Igea, J., & Glassgold, A. E. 1999, ApJ, 518, 848  
Ilgner, M., Henning, Th., Markwick, A. J., Millar, T. J. 2004, A&A, 415, 643  
Ilgner, M., Nelson, R. P., 2006, 445, 205  
Kastner, J.H., Zuckerman, B., Weintraub, D.A., & Forveille, T. 1997, Science, 277, 67  
Katz, N., Furman, I., Biham, O., Pirronello, V., & Vidali, G. 1999, ApJ, 522, 305  
Kurucz, R. 1993, ATLAS9 Stellar Atmosphere Programs and 2 km/s grid. Kurucz CD-ROM No. 13. Cambridge, Mass.: Smithsonian Astrophysical Observatory.  
Lin, S.-Y., Ohashi, N., Lim, J., Ho, P.T.P., Fukagawa, M., & Tamura, M., 2006, ApJ, 2006, 645, 1297  
Markwick, A. J., Ilgner, M., Millar, T. J., & Henning, T. 2002, A&A, 385, 632  
Müller, H.S.P., Schlöder, F., Stutzki, J., & Winnewisser, G. 2005, J. Mol. Struct., 742, 215  
Müller, H.S.P., Thorwirth, S., Roth, D.A., & Winnewisser, G. 2001, A&A, 370, L49

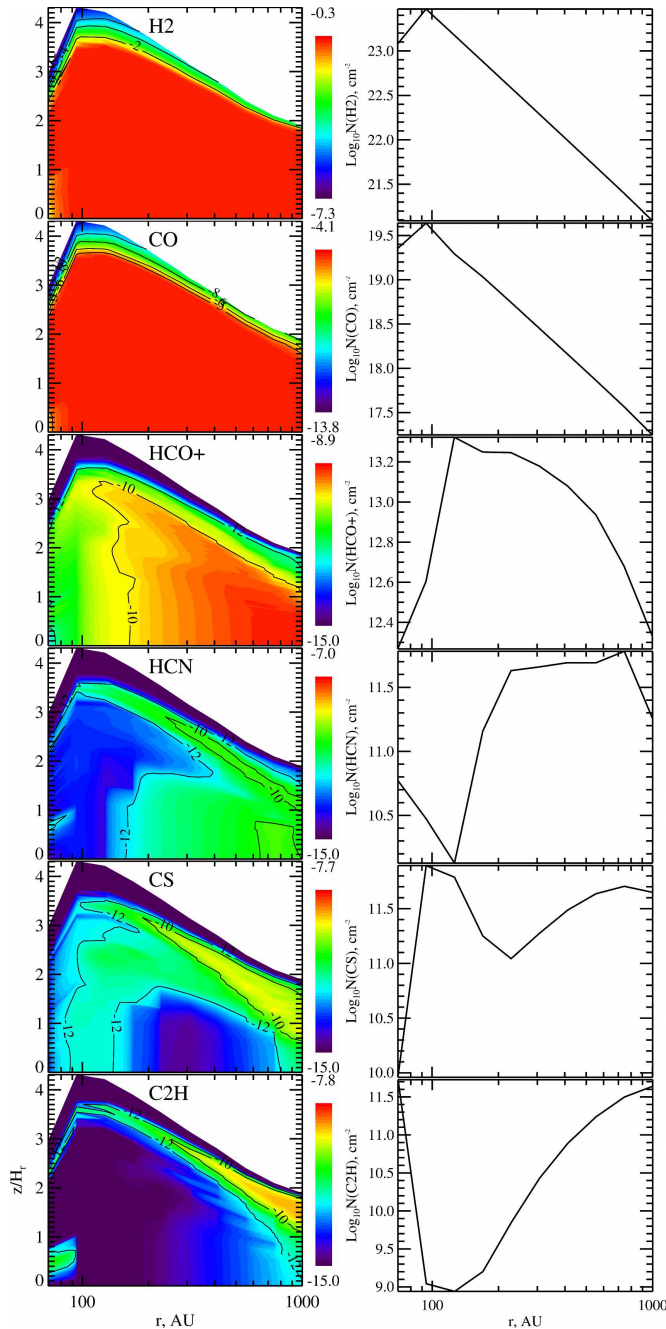


**Fig. 3.** (Left) Modeled abundance distributions in the disk of AB Aur at 2 Myr (relative to total amount of hydrogen nuclei) for H<sub>2</sub>, CO, HCO<sup>+</sup>, HCN, CS, and C<sub>2</sub>H. The vertical axis is angle in radians. (Right) The corresponding radial distributions of the column densities ( $\text{cm}^{-2}$ ).

Öberg, K. I., Fuchs, G. W., Awad, Z., Fraser, H. J., Schlemmer, S., van Dishoeck, E. F., & Linnartz, H. 2007, *ApJ*, 662, L23  
 Oka, T. 2006, *Proceedings of the National Academy of Sciences*, v. 103, N. 33, 12235  
 Pascucci, I., et al. 2007, *ApJ*, 663, 383  
 Piétu, V., Guilloteau, S., & Dutrey, A. 2005, *A&A*, 443, 945 (Paper II)  
 Piétu, V., Dutrey, A., Guilloteau, S., Chapillon, E., & Pety, J. 2006, *A&A*, 460, L43

Piétu, V., Dutrey, A., & Guilloteau, S. 2007, *A&A*, 467, 163  
 Qi, C. PhD Thesis. 2001, California Institute of Technology  
 Roberge, A., et al. 2001, *ApJ*, 551, L97  
 Rodríguez, L. F., Zapata, L., & Ho, P. T. P. 2007, *RMxAA*, 43, 149  
 Semenov, D., Wiebe, D., & Henning, Th. 2004, *A&A*, 417, 93  
 Semenov, D., Pavlyuchenkov, Ya., Schreyer, K., Henning, Th., Dullemond, C., & Bacmann, A. 2005, *ApJ*, 621, 853 (Paper I)  
 Semenov, D., Wiebe, D., & Henning, T. 2006, *ApJ*, 647, L57  
 Shakura, N. I. & Sunyaev, R. A. 1973, *A&A*, 24, 337  
 Smith, I. W. M., Herbst, E., & Chang, Q. 2004, *MNRAS*, 350, 323  
 Telleschi, A., Güdel, M., Briggs, K. R., Skinner, S. L., Audard, M., & Franciosi, E. 2007, *A&A* 468, 541  
 Thi, W.-F.; van Zadelhoff, G.-J.; & van Dishoeck, E.F. 2004, *A&A*, 425, 955  
 Tscharnuter, W. M., & Gail, H.-P. 2007, *A&A*, 463, 369  
 Turner, N. J., Sano, T., & Dziourkevitch, N., 2007, *ApJ* 659, 729  
 van den Ancker, M. E., de Winter, D., & Tjin A Djin, H. R. E. 1998, *A&A*, 330, 145  
 van den Ancker, M.E., Bouwman, J., Wesselius, P.R., Waters, L.B.F.M., Dougherty, S.M., & van Dishoeck, E.F. 2000, *A&A*, 357, 325  
 van Dishoeck, E. F., & Blake, G. A. 1998, *ARA&A*, 36, 317  
 van Dishoeck, E. F., Jonkheid, B., & van Hemert, M. C. 2006, *Faraday Discussion* 133, 231  
 van Zadelhoff, G.-J., van Dishoeck, E.F., Thi, W.-F., & Blake, G.A. 2001, *A&A*, 377, 566  
 Vasyunin, A. I., Semenov, D., Henning, T., Wakelam, V., Herbst, E., & Sobolev, A. M. 2008, *ApJ*, 672, 629  
 Wakelam, V., Herbst, E., Selsis, F., & Massacrier, G. 2006, *A&A*, 459, 813  
 Willacy, K., Klahr, H. H., Millar, T. J., & Henning, Th. 1998, *A&A* 338, 995  
 Willacy, K., Langer, W., Allen, M., & Bryden, G. 2006, *ApJ*, 644, 1202  
 Wooden, D.H., Harker, D.E., & Brearley, A.J. 2005, In: *Chondrites and the Protoplanetary Disk*, ASP Conference Series, Ed. A.N. Krot, E.R.D. Scott, & B. Reipurth. San Francisco: Astronomical Society of the Pacific, 341, 774